Differential Stone Decay of the Spanish Tower Façade in Bizerte, Tunisia

K. Zoghlami, Ph.D.[1]; P. Lopez-Arce, Ph.D.[2]; and A. Zornoza-Indart[3]

Abstract: The Spanish Fortress of Bizerte in Tunisia shows differential erosion patterns on the rock ashlars used in the construction of its main façade (sixteenth century) exposed to marine aerosol action and several restoration works. In order to determine the origin of this erosion and the degree of stone decay, a combination of microdestructive and nondestructive techniques have been used on-site and in the laboratory. Moisture measurements, ultrasonic velocity propagation, and water absorption by a Karsten pipe test, together with polarized light and fluorescence optical microscopy, mercury intrusion porosimetry, and ion chromatography analyses, were carried out to perform petrophysical characterization of stone samples and determination of soluble salts. Results show that the differential stone weathering is caused by small variations in the petrographic characteristics of the construction's geomaterials, such as the type and degree of cementation, porous network configuration, and presence or absence of soluble salts. These variations are also detected by the portable nondestructive techniques, showing their analytical sensitivity to small petrophysical changes even in the same type of rock and their performance in predicting future degradations not currently visible on the surface of the rocks. **DOI: 10.1061/(ASCE)MT.1943-5533.0001774.** *© 2016 American Society of Civil Engineers.*

Author keywords: Petrophysics characterization; Stone decay; Nondestructive techniques; Salt crystallization; Durability; Architectural heritage.

Introduction

Cultural stone weathering studies contribute substantially to the knowledge of erosion rates, revealing the importance of specific decay agents and weathering factors (Philippon et al. 1992; Winkler 1994; Croci and Delgado Rodrigues 2002; Martinez-Martinez 2011). Surface recession takes place when weathered material is removed from the rocks. In order to know how fast weathering and erosion occur when sampling is not allowed at architectural heritage sites (as in the current case), analyses using microdestructive and nondestructive techniques are applied to measure the weathering of rocks caused by physicochemical changes that occur in bedrocks (Fort et al. 2008). Salt crystallization (Angeli et al. 2007); freeze-thaw cycles (Ruedrich 2007; Martinez-Martinez et al. 2013); and thermal shock processes influenced by water, wind, temperature, or any type of environmental agent leading to weathering can be inferred by performing on-site measurements or through experimental laboratory works.

Nondestructive techniques (NDT) can be used to evaluate the performance of protective treatments for architectural cultural heritage sites by quantifying the changes in the physicochemical properties of construction and building materials (Nwaubaniand Dumbelton 2001; López-Arce et al. 2010; Herinckx et al. 2012). Since sampling is not needed, avoiding damaging valuable materials, and a higher number of results can be acquired faster, the use of in situ NDT offers several advantages. Portable nondestructive analytical equipment can be used to determine mineralogical and chemical composition of construction materials or decay products that cause damage to the surface of archeological and architectural cultural heritage sites (López-Arce et al. 2011).

Ultrasound propagation velocity has been widely used as a NDT to determine the quality and degree of decay in rock and stone materials that form part of the built heritage site (Alvarez de Buergo and Gonzàlez 1994; Price 1996; Esbert et al. 1997; Papida et al. 2000; Weiss et al. 2000; Török 2003; Vasconcelos et al. 2008).

Many investigations highlight the importance of assessing the water absorption behavior to evaluate and quantify stone decay. Several authors (Van Hees 1995; Vallet et al. 1999; Vandevoorde et al. 2013) confirm that the Karsten pipe test is a very useful tool for measuring the water absorption rate comfortably and effectively in porous rocks. Nevertheless, some difficulties and limitations are usually encountered when performing this in situ technique, such as loss of data before starting the measurements, difficulties of fixing the tube in some areas, and reduction of the contact area by the plastiline that seals the tube to the surface as recorded by Vandevoorde et al. (2013). This technique allows measuring of the liquid water permeability through a rock wall or other materials in a simple, very fast, and nondestructive way. Nevertheless, the outdoor temperature, relative humidity, and time of day also affect the results, so these variables should be taken into account when interpreting the results (Menezes et al. 2015). Equally, portable moisture meters (GE Protimeter, Survey Express Services, London, U.K.) can be used to calculate a resistivity-based parameter [wood moisture equivalent (WME%)] as an indicator of water and salt content inside rock samples, as both high moisture levels and high salt content can give high WME values (Aly et al. 2015). Massari and Massari (1993) and Tavares et al. (2005) judged this equipment as a suitable instrument for obtaining readings of the surface moisture content of several materials; when used with accuracy, this is a very

[1]Département de Geologie, Laboratoire de Ressources Minérales et Environnement, Université Tunis el Manar, Faculté des Sciences de Tunis, 2092 El Manar Tunis, Tunisia (corresponding author). E-mail: karimazoghlami@hotmail.com

[2]Deptartment of Geology, Museo Nacional de Ciencias Naturales (CSIC), C/Jose Gutierrez Abascal 2, Madrid 28006, Spain.

[3]Ph.D. Student, Restorarion of Historical Constructions, Urban Evolution and Refurbishment, H.T.S. Architecture, Univ. of the Basque Country (UPV/EHU), Plaza Oñati 2, Donostia-San Sebastian 20018, Spain.

Note. This manuscript was submitted on February 8, 2016; approved on August 4, 2016; published online on December 5, 2016. Discussion period open until May 5, 2017; separate discussions must be submitted for individual papers. This paper is part of the ***Journal of Materials in Civil Engineering***, © ASCE, ISSN 0899-1561.

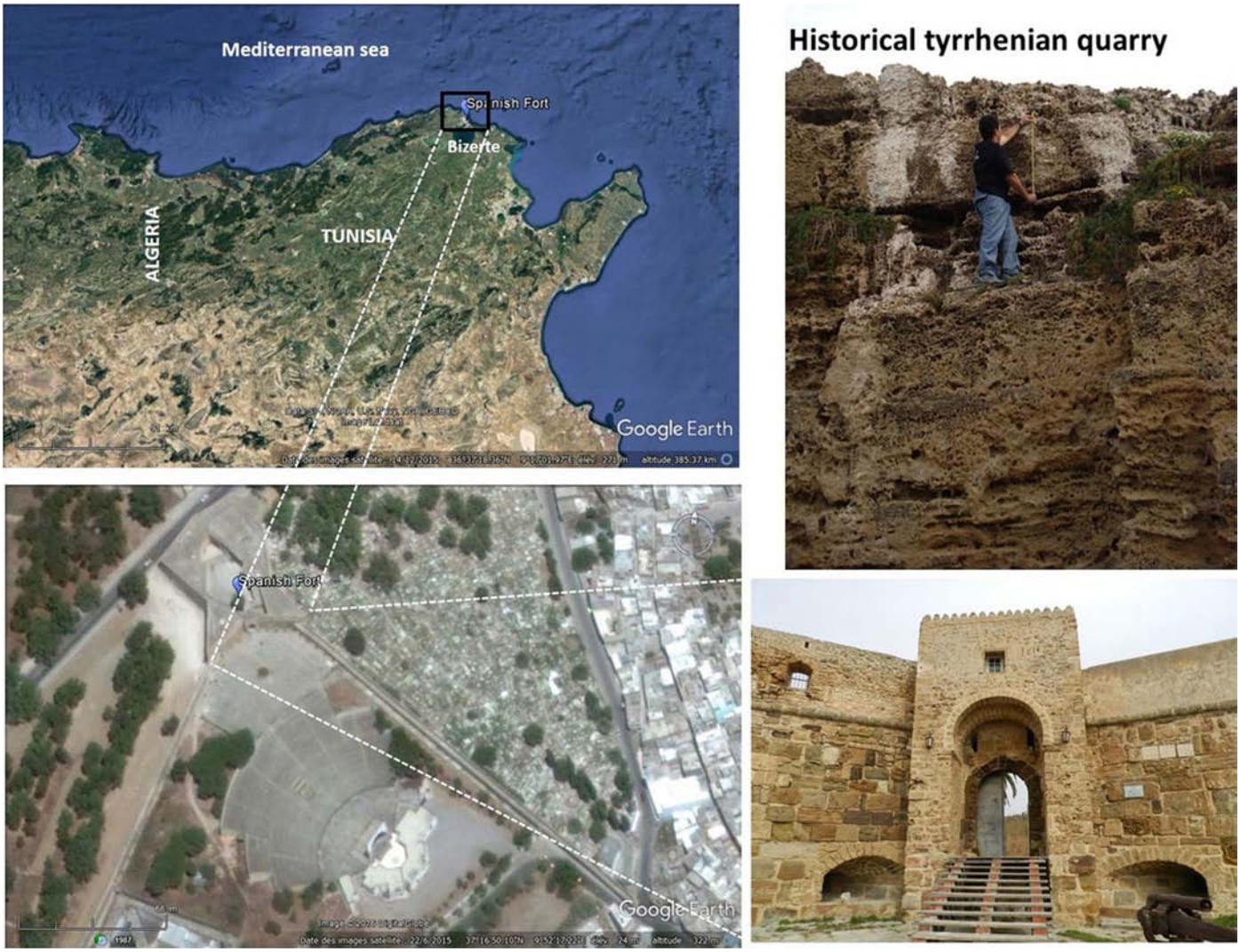

Fig. 1. Location map of the Spanish Tower of Bizerte, Tunisia (Map Data: Google, SIO, NOAA, U.S. Navy, NGA, GEBCO, Image Landsat, Image © 2016 DigitalGlobe)

useful tool for the detection of areas of high moisture content. However, the obtained values can only be used as a comparative analysis (Flores-Colen et al. 2011; Duarte et al. 2011). In addition, by performing several measurements on a wall surface, it is possible to plot a distribution map of surface moisture content (Burkinshaw 2002). The weather conditions also greatly affect the results. So, outdoor walls after rain present higher results than in dry weather conditions. The state of degradation of building materials, such as the presence of stains or biological colonization, also affects the results (Duarte et al. 2011; Menezes 2012; Tavares et al. 2005).

However, for a more accurate determination of the physicochemical properties of these materials, collecting small samples and further laboratory analyses are sometimes required.

For example, the rock-cut façades at the Archaeological Park of Petra in Jordan show a high presence of sodium chloride that is not detectable with a portable micro-Raman, so it is necessary to collect samples and analyze them in the lab to identify the origin of the soluble salts that are causing weathering of the monuments by salt crystallization processes (López-Arce et al. 2011). Recent technological developments in the field of NDT have enhanced their usefulness in the field of built cultural heritage site protection, and they are indispensable tools for the characterization of materials, detection of weathering and degradation, assessment of intervention effectiveness, and evaluation of compatible materials and processes (Moropolou et al. 2013). In situ experimental comparative tests carried out by Andreini et al. (2014) on stone masonry walls performed in the Volterra in Pisa, Italy, consisted of using microdestructive and nondestructive tests with multiple purposes to show the petrophysical variability of the building materials and the influence of atmospheric weather conditions on the measured parameters.

The objective of this work is to study the origin of differential stone decay in the Spanish Tower of Bizerte to establish the differences in weathering and durability processes. This information is necessary to propose better solutions for preservation and restoration practices adapted to the intrinsic characteristics of these stone building materials. Based on the previous literature review and the current problems to solve, a combination of microdestructive and nondestructive techniques have been selected to carry out this research work.

Experimental

Building Materials

The Spanish Tower of Bizerte is a major bastion of the sixteenth century situated on the top of the hill El Kodia in Bizerte Tunisia

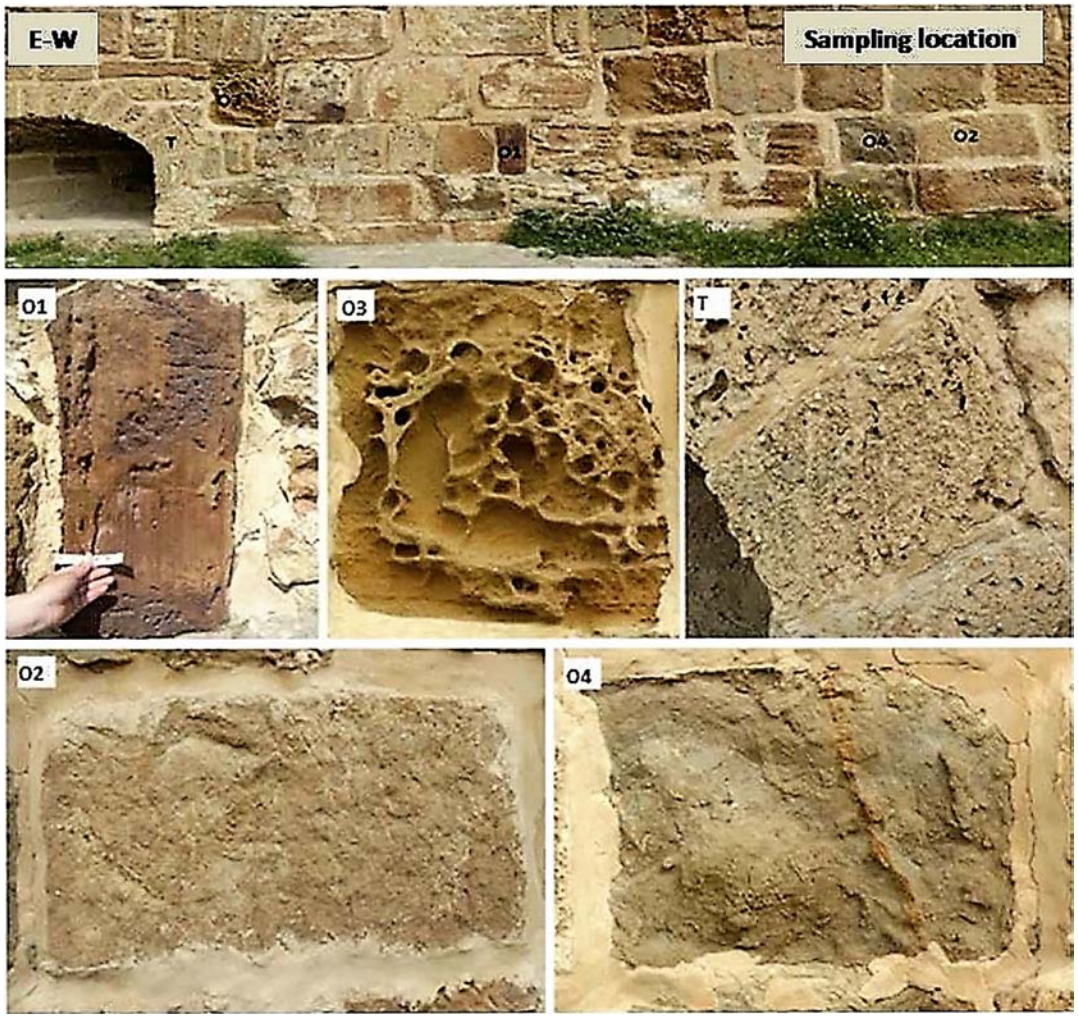

Fig. 2. Front façade wall of the Spanish Tower of Bizerte showing sampling locations and details of the five studied stone ashlars

(Fig. 1). This name, which is in fact inadequate, seems to attribute the construction of this fortress to the Spanish people who had occupied the city from CE 1535 to 1573. However, it was the Pasha of Algiers Eulj Ali, who ordered its construction in CE 1570, but he had no time to finish it when his troops were expelled from Bizerte (Bouita 1992). Originally the monument was built of rammed earth with the exception of the south façade, which was built with stone.

The monument is located a few hundred meters from the sea and its western façade is directly exposed to the traffic. The north and east façades are oriented to the sea. The south façade, which is the object of this research, gives panoramic views to the medina of Bizerte town.

The monument has undergone different historical restoration works, which unfortunately have not been documented. The most important one corresponds to the French colonial era, which essentially consisted in covering the earlier walls built with rammed earth. More interventions have been carried out and primarily consisted of replacing the bedding mortar joints. Replacements of rock ashlars was limited to some areas that were probably severely damaged.

The main façade of the fort is constructed with stone ashlars of several dimensions, with different colors and textures, at least from a macroscopic point of view. Each lithotype displays a different degree and type of weathering pattern (Fig. 2).

The building materials are Oligocene sandstones and Quaternary calcarenite. Sandstone outcrops are located in a very restricted area of Bizerte's city, such as the hill of El Kodia where the studied monument stands, but the historical quarries have not yet been found. The Quaternary calcarenite outcrops around the entire northern coast of Bizerte have been studied by Zoghlami and Gomez Gras (2009) (Fig. 1). These are from the Eutyrrhenian to Würm geological periods, and they are generally represented by the Rejiche, Chebba, and Cap Blanc formations (Paskoff and Sanlaville 1983).

Within these geological formations, historic quarries were opened in the past to supply building stones to a large number of Bizerte's monuments.

Five representative lithologies of these building materials used in the construction of the main façade of the fort, named as samples O1, O2, O3, O4 (from the Oligocene age), and Sample T (Quaternary calcarenite), were studied in this work. Two ashlars of each one of these five lithologies were selected for on-site measurements and sampling for further laboratory analyses (Fig. 2). The measurement areas were chosen on the basis of accessibility and homogeneity of the stone surfaces to avoid large variations of the petrophysical measured values.

Field Tests

Moisture content on the stone surfaces was measured with a portable moisture meter (GE Protimeter Surveymaster, Survey Express Services, London, U.K.) by penetrating pins (resistance sensor).

Fig. 3. On-site measurements with nondestructive techniques: (a) measurements of moisture content; (b) water absorption measurements by Karsten pipe; (c) sampling of stone powder by means of an electrical drill to perform further soluble salt measurements by ion chromatography analyses; (d) ultrasonic velocity (V_p) measurements

The nominal depth of the measurement was 19 mm (3/4 in.), although this depended on the density and other characteristics of the material. Depending upon the moisture reading, one of the LEDs will light up to allow the surveyor to read the moisture reading. When reading the damp measurement using the two pin mode (measure), the scale runs from 7 to 99% wood moisture content (WMC). The %WMC has become an industrially recognized reading for moisture whether the material is wood, brick, stone, or concrete. When reading the damp measurement using the search mode, the scale runs from 0 to 999 WME [Fig. 3(a)]. Depending on the dimension on the ashlars, from 8 to 16 measurements were performed (Fig. 4). The obtained results were processed with *Surfer* software to obtain moisture distribution maps of the studied rock ashlars.

Ultrasonic velocity (V_p or *P*-wave velocity) was measured to assess the compaction of the different lithologies. *P*-wave propagation time was measured to a precision of 0.1 μs with a PUNDITCNS Electronics US instrument (CNS Farnell, Winslow, Buckinghamshire, U.K.). The frequency of the transducers used was 1 MHz. The diameter of the flat contact area on these transducers was 11.82 mm. The bond between the transducers and the surface of the specimens was secured with a carboxymethylcellulose paste (Sichozell Kleister, Henkel). Measurements were taken in indirect transmission/reception mode with a distance between transducers of 5 cm [Fig. 3(d)]. The obtained results have been processed with *Surfer* software to obtain Vp distribution maps of the studied rock ashlars. From 8 to 16 measurements were performed depending on the size of each ashlar (Fig. 4).

Water absorption tests were carried out using a Karsten pipe (KT) (TQC, Germany) according to the RILEM standard [RILEM 25-PEMRILEM 1980)] and the methodology described by Vandevoorde et al. (2013), after introducing some modifications to overcome difficulties encountered during in situ measurements. The water absorption rate was measured by introducing 4 mL of water (Karsten pipe volume) [Fig. 3(b)] and noting the quantity of water absorbed at 30-s intervals. In this case, the authors chose to fix the quantity of water because it was very difficult to re-establish the water level, especially for the lithotype *T*. So, to calculate the absorption rate, the same amount of water for the five lithotypes was introduced in the Karsten pipe. The absorbed quantity was noted at the same time intervals to have enough data to plot the results. Measurements were recorded once the water was poured into the tube to avoid loss of data. In order to improve the fixing of KT to rough stone surfaces, a puttylike pressure-sensitive adhesive made of a synthetic rubber (similar to Blu-tack type) was used. The results are represented in curves where the slopes correspond to water absorption rates in each case.

Laboratory Analyses

Thin sections were prepared from samples of stone fragments collected from the ashlars and these were studied under polarizing light optical microscopy (PLOM) to study the petrography. Fluorescence optical microscopy (FLOM) was also carried out on the same samples and on the same areas previously pictured by PLOM. The samples were impregnated with epoxy resin mixed with fluorescence in order to observe porosity under fluorescent light under the same petrographic microscope. Thirty-μm-thin sections of the stone samples were prepared and dyed with alizarin red to distinguish calcite from dolomite. These thin sections were studied with an Olympus BX51 polarized light optical microscope fitted with an Olympus DP 12 (6 V/2.5 Å) digital camera.

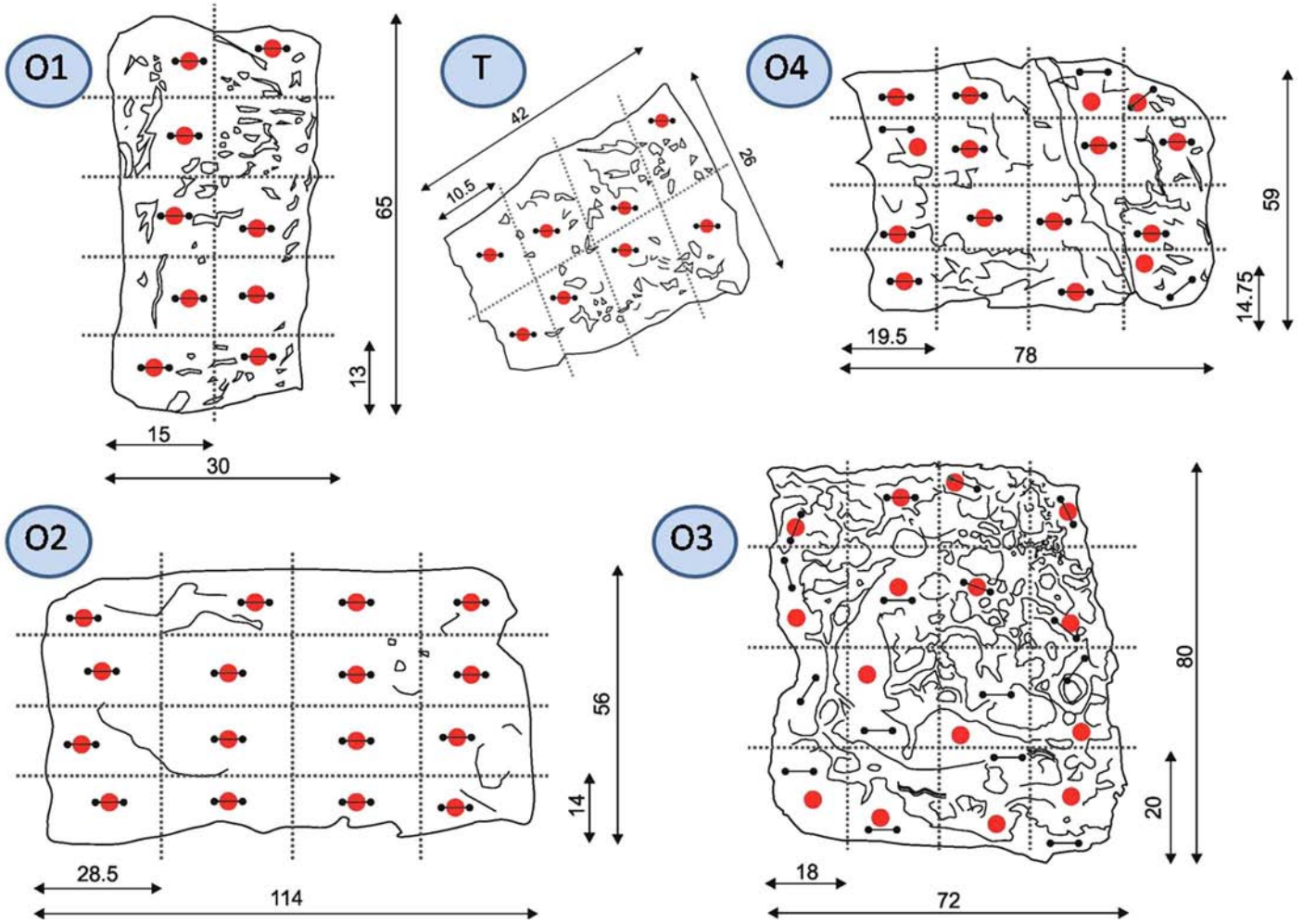

Fig. 4. Sketches of the studied stone ashlars showing the NDT measurements' positions: position of the KT measurements (big red points); position of the moisture meter and transducers of the ultrasonic equipment (small black points)

Fragments of each lithology were also collected to perform mercury intrusion porosimetry analyses to determine the total porosity and pore size distribution. Readings were taken in the range of pore diameters between 0.005 and 400 μm under measuring conditions ranging from atmospheric pressure to 228 MPa (60,000 psia). Stone sample cores with a diameter of 10-mm and a height of at least 30 mm were cut and analyzed with a Micromeritics Autopore IV 9500 MIP (Micromeritics, Norcross, Georgia).

NDT measurements were performed on selected stone ashlars by drilling with an electric drill at different depths (1, 3, and 5 cm from the surface) [Fig. 3(c)]. Only one test per lithotype was carried out and the stone ashlars were drilled in the center to avoid as much as possible the influence of the bedding mortar surrounding the ashlars. At each depth the stone powder generated by drilling was extracted and then the collected samples were analyzed by ion chromatography (IC) to quantify the type and concentration of soluble salts (ions) present in the drilled materials. Anions (Cl^-, NO_3^-, SO_4^{2-},F^-, nitrites, and oxalates) were determined in all the samples. Anion concentrations served to study the concentration of soluble salts with stone depth. The method used for extracting soluble salts was based on an alternative to the method described in the NORMAL standard with some additional modifications (Iñigo et al. 2001). Approximately 0.1 g of powdered stone samples was dissolved in 10 mL of Milli-Q ultrapure water and placed for 45 min in an ultrasonic bath at ambient temperature. They were subsequently centrifuged for 5 min at 3,500 rpm and a centrifugal force of 3,400 rfc. The soluble salts (anions) in the extracted samples were quantified on a Metrohm 761 Compact IC ion chromatograph (Metrohm, Switzerland).

Results

Field Tests

Moisture Measurements

Moisture values in all the ashlars range from 10 to 30% WME. The lowest values correspond to the lithology of Sample T ($10.26 \pm 3.65\%$), which corresponds to the driest one, while the highest value corresponds to the lithology of O4 ($30.50 \pm 7.15\%$), which is the wettest one.

The other lithologies display intermediate and similar moisture values: Sample O1 has $21.42 \pm 2.46\%$, Sample O2 has $24.81 \pm 7.22\%$, and Sample O3 presents $21.57 \pm 5.31\%$.

In Samples O1 and O2, moisture levels are more homogeneously distributed along their respective ashlars, meaning that these are almost totally dry on their entire surface, whereas for Samples O3 and O4, moisture concentrates in selective areas (Fig. 5).

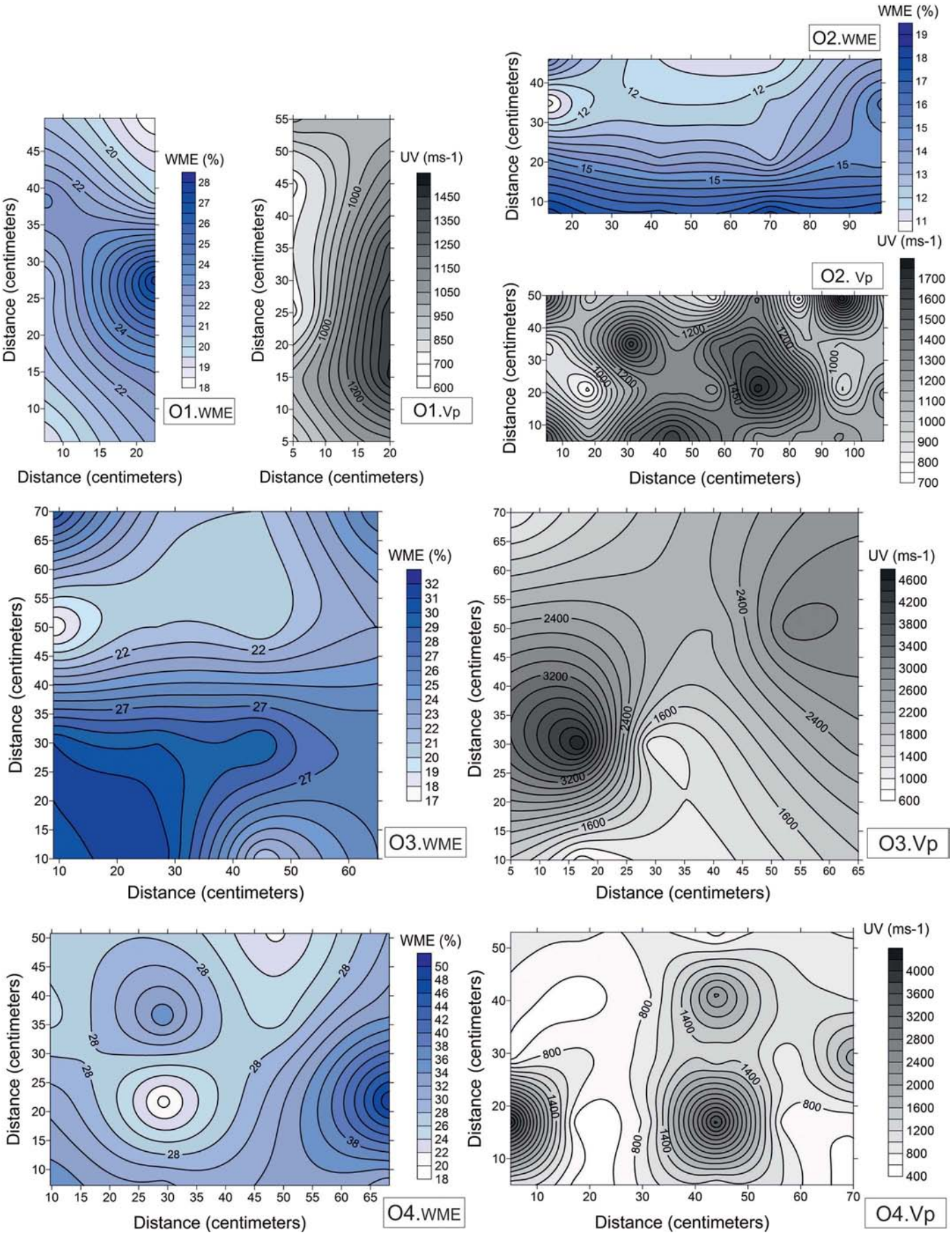

Fig. 5. Moisture levels (%WME) and ultrasonic velocity values UV (V_p in m/s) distribution maps of the stone ashlars that correspond to lithologies O1, O2, O3, and O4

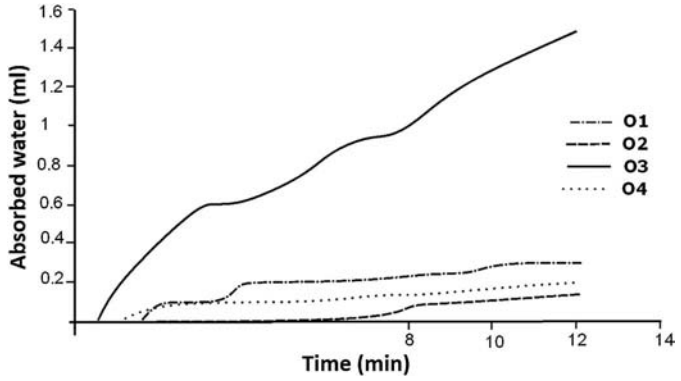

Fig. 6. Water absorption curves obtained by the Karsten pipe in stone ashlars of four studied lithologies of the Spanish Tower façade of Bizerte

Ultrasonic Velocity Propagation

The values of the five lithologies range between $1{,}580 \pm 57$ m/s (Sample T) and $3{,}801 \pm 29$ m/s (Sample O1). Samples O3 and O4 reach values around 3,000 m/s ($3{,}062 \pm 208$ m/s and $3{,}142 \pm 56$ m/s, respectively). The larger standard deviation of Sample O2 ($2{,}017 \pm 273$ m/s) compared to the other samples could be a result of the greater differences in the moisture content within the ashlar where the ultrasonic measurements were taken in the same spots. Velocity values were heterogeneously distributed along the entire surface of the different ashlars, as shown in Fig. 5.

Water Absorption by Karsten Pipe

Fig. 6 shows the water absorption curves obtained by means of a Karsten pipe tool in representative stone ashlars of the studied lithologies.

Sample T (calcarenite) has an extremely rapid absorption rate (this is why it is not represented in the curves). The absorption time of the total amount of water inside the pipe (4 mL) was only 6 s (40 mL/min).

The other sandstone samples have much slower water absorption rates, i.e., Sample O3 (0.116 mL/min) followed by Sample O1 (0.025 mL/min). Samples O2 and O4 have the slowest absorption rates and therefore the slowest absorption coefficients (0.014 mL/min).

Laboratory Studies

Polarizing Light and Fluorescence Optical Microscopy

The petrographic characteristics of the studied samples are described as follows.

Lithotype (T) is a highly porous bioclastic calcarenite, partially cemented by calcite. The porosity is much more connected than in the other samples. The detrital fraction is essentially represented by quartz and rock fragments (Fig. 7).

Sample O1 is sandstone primarily composed of monocrystalline quartz; compaction is very low, with almost no concave-convex contacts. The rock is largely cemented by iron oxide. The intergranular porosity is characterized by high connectivity [Fig. 7(c)].

Sample O2 is sandstone essentially composed by quartz with syntaxial cement. The rock is iron oxide cemented but this cement is less abundant than in the previous sample. There is also a fraction of calcareous cement. The rock is very compacted with quartz grains characterized by frequent concave-convex contacts. The calcareous cement is ankerite $[CaFe(CO_3)_2]$ (blue-violet dyed). The type of porosity is similar to that of Sample O1.

Sample O3 is sandstone mainly composed of quartz. This is a very compacted rock cemented by iron oxide. No petrographic or mineralogical differences were detected between Samples O2 and O3.

Sample O4 is sandstone primarily formed by quartz and bioclasts (nummulites), bivalves, and gastropods. The rock is cemented by calcium carbonate (essentially calcite) with highly developed sprite crystals. Early cementation occurred, since there are almost no contacts among the different components of the rock. Porosity is primarily of fissured type (Fig. 7).

Mercury Intrusion Porosimetry

In Table 1 are summarized the main characteristics of the pore network analyses and in Fig. 8 the pore size distribution curves of the five studied lithologies are shown.

The most porous rock is the calcarenite (Sample T), with 40.10% total open porosity accessible to mercury, followed by Sample O1 (22.08%) and then Sample O2 (20.52%). The others lithologies display lower similar values (17.24% for Sample O3 and 17.25% for Sample O4). All these lithologies have a large microporous portion except the calcarenite sample. This microporosity [pores with a diameter below 5 μm (Russell 1927; Gomez-Heras and Fort 2007; Fort et al. 2013)] is highly developed in Sample O1, while macroposity (>5 μm) is much more significant in Sample T.

The pore size distribution is very similar in all lithotypes except for Samples O1 and T, which are quite different. Even though both samples have a general polymodal distribution, the *T* sample displays most of its porosity above 10 μm, while in Sample O1 most of its porosity is represented by a bimodal distribution with pore diameters in the range between 0.1 and 1 μm and in the range between 1 and 10 μm.

Ion Chromatography

Table 2 compiles the type and concentration of soluble salts obtained by ion chromatography analyses.

Sample O3 is the lithology that contains the largest amount of soluble salts followed by Samples O4 and O1, and then Sample O2 followed by Lithotype T with a negligible content.

The main types of salts presenting the different lithologies are mainly chlorides, nitrates, and sulphates. Sample O1 contains the highest chloride concentration (133.8 mg/L) and low sulphate concentration (17 mg/L). It also has a significant content of nitrates (111.2 mg/L), although slightly lower than that of Sample O4, which has a quite high chloride content (96.7 mg/L) and very high amount of sulphates (435.4 mg/L).

Sample O3 shows the highest amount of sulphates (959.7 mg/L) with relatively high levels of chlorides and nitrates. Samples O2 and T display the lowest total salt content, even though Sample O2 has 92.8 mg/L of sulphates.

Fig. 9 shows the graphs with the anion salts content (chlorides, nitrates, and sulphates) obtained in the stone ashlars. In all cases a decrease in depth of the amount of salts can be observed, which indicates that the salts are mostly concentrated at the surface of the ashlars.

Discussion

A comparison of the different petrophysical characteristics of the studied lithologies (Table 3) shows that Samples O2 and O3 are alike since they have similar mineralogical and petrographic features. In spite of ultrasonic velocity results, they display equally similar physical properties, porosity, and pore size distribution values. Despite these similarities, Lithotype O3 shows an advanced alteration degree compared to Sample O2. This fact explains the

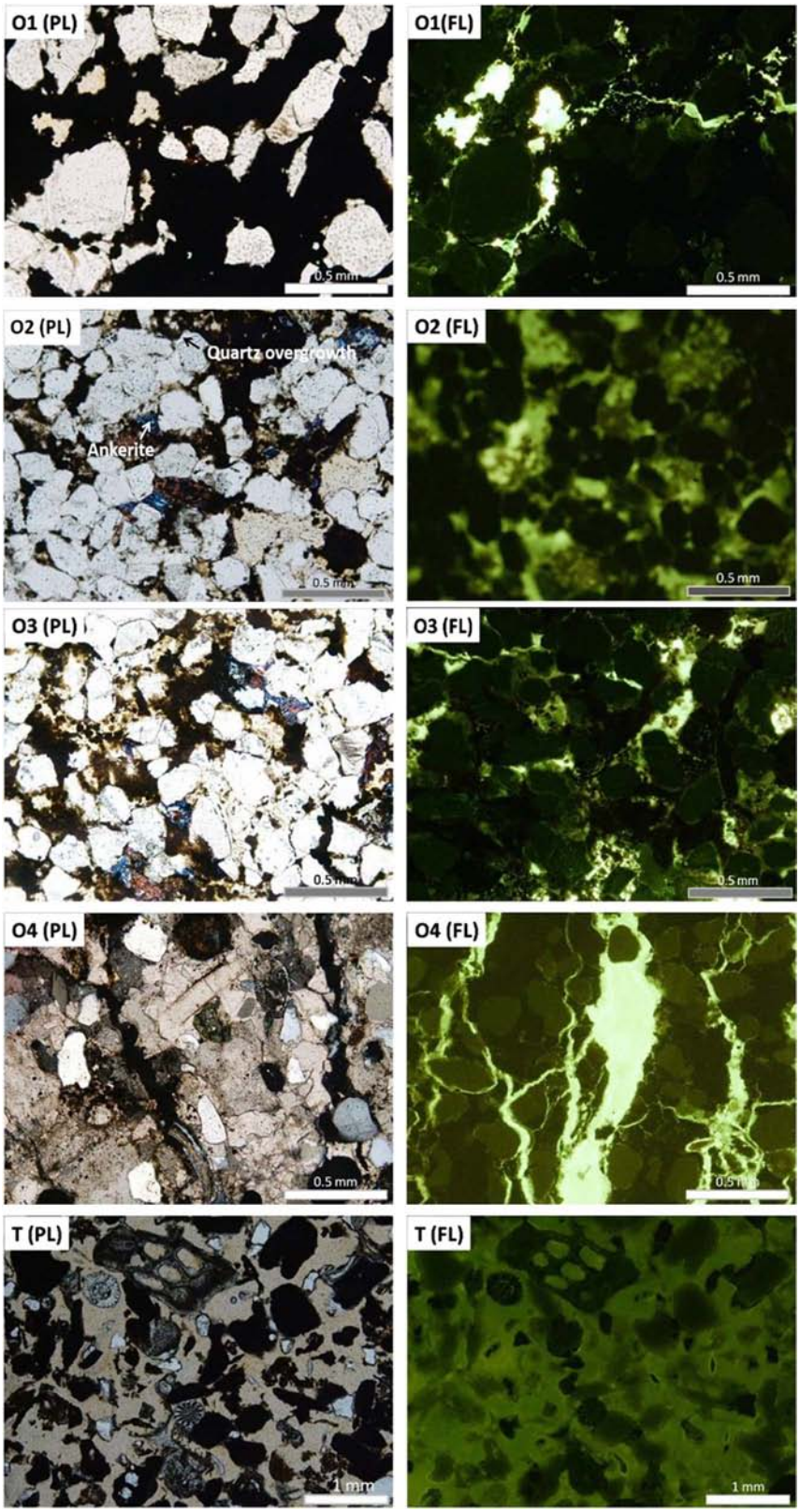

Fig. 7. Polarizing light (PL) and fluorescence light (FL) optical microscopy images obtained with ×10 magnification

differences obtained between Samples O2 and O3 in the ultrasonic and water absorption rate values. From the ion chromatography results of both lithologies (Table 2), it can be inferred that the higher velocity values and at the same time, a higher degree of alteration of Sample O3 observed on-site, is a result of its higher salt content, especially sulphates (Goudi 1999; Simon and Lind 1999). It seems that Sample O3 has the same lithology as Sample O2, but after weathering. Taking this into account, the results from the analytical characterization of Samples O1, O2/O3, and O4 can be compared as follows.

Table 1. Main Pore System Characteristics Obtained by Mercury Intrusion Porosimetry of Each Lithology

Samples	Total connected porosity (%)	Pore size (diameter) distribution (%)					
		<0.01 μm	0.01–0.1 μm	0.1–1 μm	1–10 μm	10–100 μm	>100 μm
O1	22.08	1.58	8.76	27.80	42.70	12.10	7.07
O2	20.52	0.59	11.69	17.00	38.76	28.70	3.27
O3	17.24	0.03	11.99	17.09	46.21	21.87	2.82
O4	17.25	0.18	6.06	15.74	41.33	33.32	3.36
T	40.10	0.27	4.13	6.77	10.36	68.35	10.12

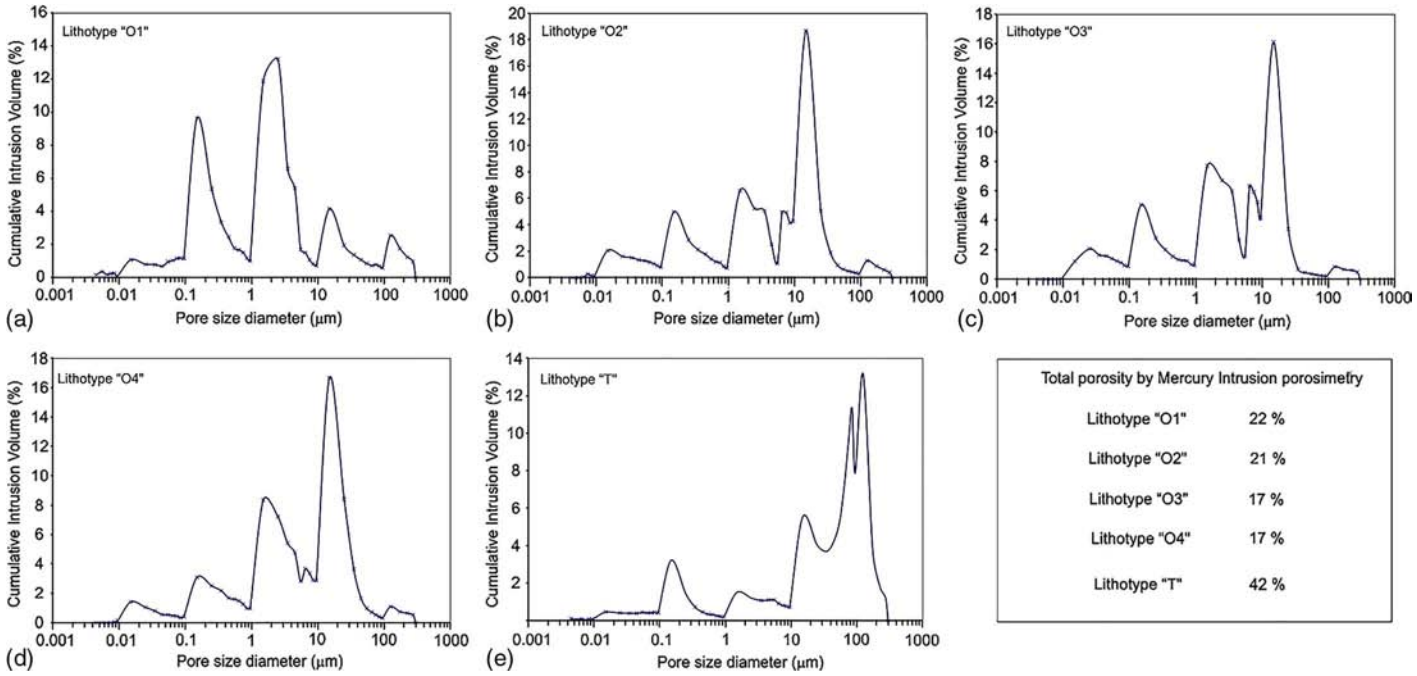

Fig. 8. Pore size distribution (PSD) obtained by mercury intrusion porosimetry (MIP) in four of the studied samples

Table 2. Type and Concentration of Soluble Salts Obtained by Ion Chromatography Analyses Performed from the First Centimeter Drilled through the Stone Surface

Samples	Fluoride (ppm)	Chloride (ppm)	Nitrite (ppm)	Nitrate (ppm)	Phosphate (ppm)	Sulphate (ppm)	Oxalate (ppm)	Total salt content (ppm)
O1	0.26	133.80	0.00	111.21	0.00	17.11	1.02	263.4
O2	0.27	1.58	0.00	1.42	0.00	92.75	1.42	97.44
O3	0.29	88.29	2.48	78.99	0.00	959.74	0.00	1,129.79
O4	0.11	96.72	0.00	121.05	0.00	435.36	2.40	655.64
T	0.14	0.31	0.00	0.22	0.00	1.41	0.00	2.08

In spite of the similar porosity presented by all lithotypes, the Oligocene Lithotype O3 shows the greatest water absorption capacity caused by its advanced weathering degree. However, water absorption values of Sample O1 are also higher than those obtained in Samples O2 and O4 because of its higher total porosity (Table 1).

On the other hand, Sample O1 and Sample T display opposite physical behaviors. These are characterized by a large and a very small proportion of microporosity and by slow and very fast water absorption rates, respectively. So, in this case, the higher amount of microporosity, the slower the rate of water absorption.

By comparison of petrographic characteristics and the state of conservation of the different studied lithotypes, the type and abundance of rock cement plays an important role in the alteration process. Lithotypes O1 and O3 only differ in the amount of iron oxide, whose concentration is larger in Lithotype O1. It can be observed that apparently to the naked eye, and from the petrophysical results, that Lithotype O1 has a better state of conservation than Lithotype O3.

A comparison of the O1 and O4 samples, which mainly differ in the type of cement composition, reveals that the O4 lithotype, cemented by carbonates, is much more weathered than the lithotype cemented by oxide iron (Sample O1).

The lower the iron cement, the greater the weathering and the lower the propagation velocity. However, Samples O3 and O4, which are visually the most weathered samples by salt crystallization processes, have the lowest total porosity percentages displaying high ultrasonic velocity propagation values. This may partially be a result of their higher salt content that blocks the pores and at

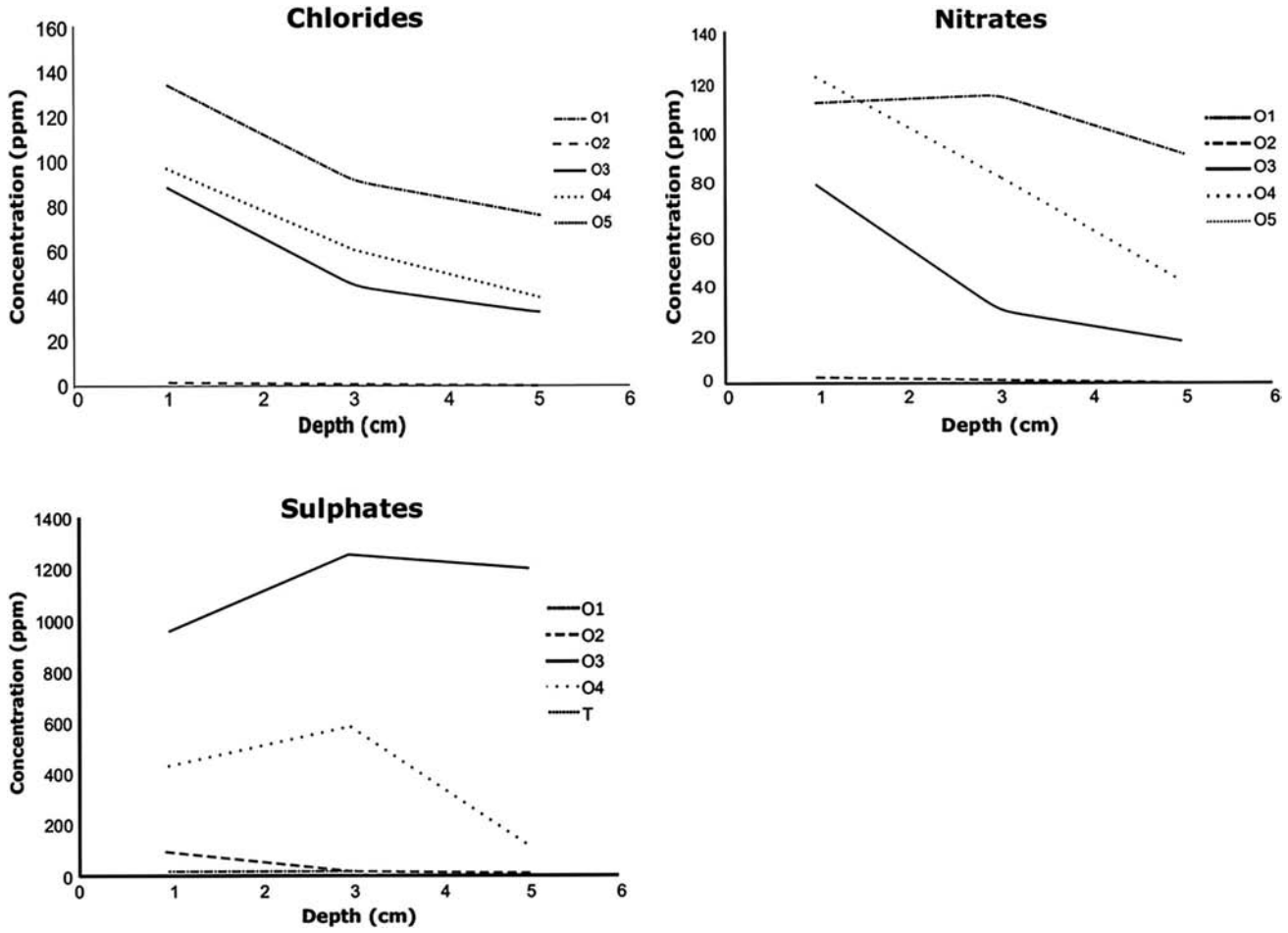

Fig. 9. Soluble salt content obtained by ion chromatography analyses from drilled samples collected at different depths from the surface of the stone ashlars

Table 3. Comparative Results of the Petrophysical Characterization Obtained with the Different Analytical Techniques of Each Studied Lithology

Sample	Total porosity (%)	Pore size distribution		Moisture level (WME%)	Water absorption (mL/min)	Ultrasonic velocity (m/s)	Total salt content (mg/L)
		<5 μm (%)	>5 μm (%)				
O1	22.08	75.1	24.9	21.42 ± 2.46	0.025	$3{,}801.55 \pm 29.21$	263.4
O2	20.52	48.6	51.4	24.81 ± 7.22	0.014	$2{,}017.03 \pm 273.15$	97.44
O3	17.24	52.2	47.8	21.57 ± 5.31	0.116	$3{,}062.73 \pm 207.83$	1,129.79
O4	17.25	47.7	52.3	30.50 ± 7.15	0.014	$3{,}142.76 \pm 56.20$	655.64
T	41.75	16.0	84.0	10.26 ± 3.65	40.00	$1{,}580.07 \pm 57.25$	2.08

the same time causes a higher weathering degree of these lithologies. The increase of the ultrasonic velocity propagation as a result of the filling of the stone pores by salts has been reported in different works. Calleja et al. (1989) pointed out an increase of ultrasound speed after subjecting limestones to a salt crystallization test. Min et al. (2005) studied the durability of building stones (granites, limestones, marbles, and basalts) exposed to a salt crystallization test, concluding that the filling of stone pores with salt crystals causes the increase of ultrasonic velocity during the early stage of salt crystallization and then, in later stages, the repeated cycles of salt crystallization result in the development of cracks, leading to a decrease of ultrasonic velocity for some rock samples. Cardell et al. (2008) applied the ultrasonic transmission technique to altered stones (limestones) by salt crystallization (single- and mixed-sulphate solutions) without extracting the salt with the aim of evaluating the binding or disintegrating effect of the different solutions on the stones and characterizing the effect of salts precipitated inside the porous media on the speed of the ultrasonic waves. The result was an increase in ultrasound speeds after subjecting limestones to a salt crystallization test, suggesting that the improvement is a result of the binding action of the subfluorescences. Their results also show that the moderate development of subfluorescences from weakly saturated solutions causes a binding effect in the calcarenite, whereas subfluorescence precipitation from highly concentrated saline solutions has a disintegrating effect, leading to break-up of the stone. Bromblet et al. (2012) also reported an increase in the in situ ultrasound speed in a study of the degradation of marble columns in the cloister of the church of Saint-Trophime in Arles, France, because of the partial filling of the pores with soluble salts. In studies of anisotropy, different authors have reported a lower structural anisotropy in samples as a result of performing a salt crystallization test before washing the

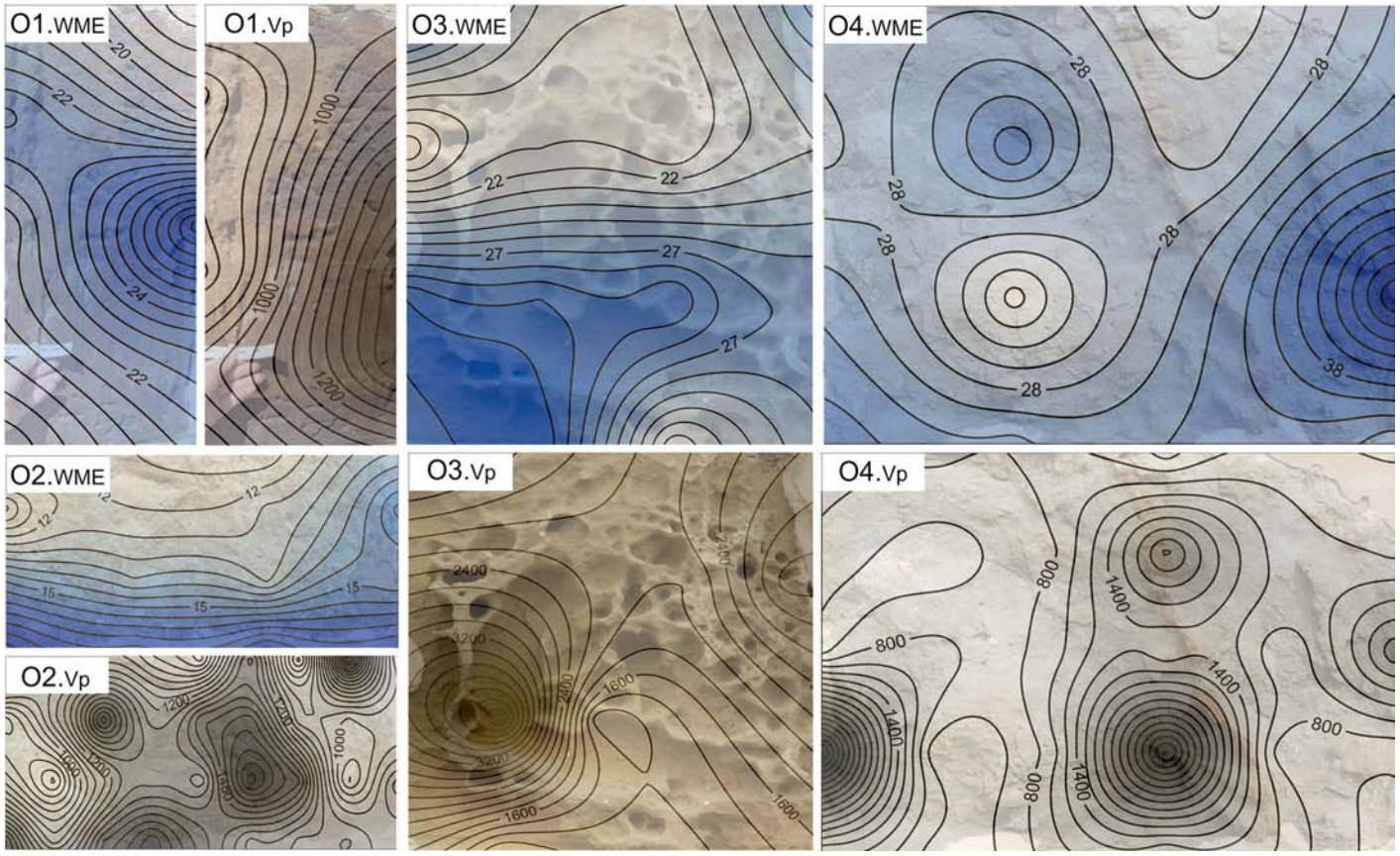

Fig. 10. Distribution maps of ultrasonic velocity (V_p in m/s) and moisture measurements (%WME) from Fig. 5, superimposed on the top of the pictures of the studied stone ashlars

samples, suggesting that salt crystals filled the discontinuities and pores of the substrates, resulting in a temporary reduction in anisotropy (Padida et al. 2000; Kramar et al. 2010).

Lithology T (calcarenite), with a different mineralogical composition, characterized by bioclasts and quartz aggregates partially cemented by calcite, has very different petrophysical characteristics. The rock is characterized by a high total porosity with a large amount of macroporosity. These petrographic characteristics give rise to very fast water absorption and desorption rates, inducing almost no water retention inside the pore system, which explains their very low salt content. However, it displays a very well-developed weathering pattern of honeycomb type. Although the term continues to cause controversy because some authors point to its origin factors such as wind erosion, temperature changes, exfoliation, freeze-thaw, salt crystallization, microorganisms, or chemical alterations, moisture and salt crystallization are today the key factors considered in the development of this type of degradation. The deterioration of the surface is from the disintegration of the mineral grains as a result of water evaporation and crystallization of the salts in the stone surface by sea spray (Mustoe 1982). An increase of connected porosity and hence a rise in the water absorption rates usually occurs after salt crystallization processes. In theory, and in terms of petrophysics and petrography, Lithotype T is the most fragile and apparently the most altered in the past by weathering agents. However, currently, because of its low amount of salts and its favorable hydric properties, this rock can be considered a quite stable lithotype in spite of its fast erosion rate by a honeycomb process.

In all the lithotypes, salt content decreases withdepth, which indicates that salts are mostly concentrated at the surface, and their probable origin is the marine aerosol. Ashlar O3 shows an increase in sulphate content with depth, which can explain its advanced degree of decay. However, a physicochemical salt contribution from dissolution-precipitation processes from the mortars used in past restorations cannot be disregarded. Chlorides, sulphates, and nitrates are typical salts found in weathered building materials affected by rising damp from salty environments (López-Arce et al. 2009a), but mortars with high levels of sulphates have been frequently used in the restoration works of historic buildings, which could have accelerated the weathering processes (López-Arce et al. 2009b). Also, in this case study portland cement has been frequently used in previous restoration works, which can partially explain the origin of sulphates in most of the stone ashlars.

The ultrasonic velocity distribution maps of the different studied lithotypes show a heterogeneous distribution of the V_p values (Fig. 5). This indicates a differential mechanical resistance (compacting degree) through the same ashlar.

A comparison of the maps of moisture and ultrasonic velocity of the studied ashlars shows no real correlation. In theory, ultrasonic velocity should increase as a function of the humidity content (Gupta and Rao 1998; Kahraman et al. 2007; Vasconcelos et al. 2008), but in this case the relationship is not evident. This can be a result of the salt content and its heterogeneous distribution in each ashlar, which influence the ultrasonic velocity values (Figs. 5 and 10).

Fig. 10 shows the superposition of distribution maps with the ultrasonic velocity and moisture measurements on top of the studied stone ashlars. The areas with the highest humidity contents are the most damaged areas, especially in Lithotypes O3 and O4 where the differential decay is well pronounced. Also, areas with high ultrasonic velocity overlap areas with largest decay, which seems

incoherent, but this can be explained as in the aforementioned paragraph, by the highest salt content in such areas. In Lithotypes O1 and O2, since they are still in a good state of conservation, the areas with high moisture content may indicate high sensibility to decay areas. Nevertheless, areas with high ultrasonic velocity values can indicate low decay degree or high salt concentration areas, which imply a future development of differential weathering inside these ashlars. The obtained distribution maps based on the NDT results can help prevent future weathering processes and identify preventive measures to preserve the stone.

So, the combination of destructive and nondestructive techniques provides much more information on the materials' physicochemical, mineralogical, and petrophysical characterizations and avoids the collection of large sample quantities of historical building materials.

Conclusions

The essential factor that controls the degree of decay of the rocks used as stone building material in the studied historic building is primarily the type of mineralogical composition and porosity, which is closely related to the hydric behavior and salt content. The original iron oxide cementation generated during its geological formation gave rise to a greater resistance to degradation by salt crystallization processes. The larger amounts of iron oxide cement the higher rock resistance. In regards to porosity, in this case, the higher amount of microporosity (<5 μm), the slower the water absorption rate, whereas the larger amount of and more connected the macroporosity (>5 μm), the faster the water absorption and desorption rates, which causes lower salt content over a longer period.

The degree of weathering in the studied lithotypes is tightly related to the salt content in the rocks. The higher total amount of salts, the higher the degree of current weathering. The type of salt can affect the degree of decay. Stone ashlars with the highest concentration of sulphate salts are more deteriorated, whereas those with lower concentrations are better preserved, such as Lithotype O1 composed of an iron cement. It seems that those cemented lithotypes are more resistant to sulphate attack, which can also be related to their higher mechanical strength and type of porosity. However Lithotype O3 displays an advanced honeycomb weathering and higher amount of sulphate salts.

In the main façade of the historic building, the decrease of salt content with depth indicates that salts are mostly concentrated at the surface of the stone ashlars and that their probable origin is marine aerosol. However, a contribution of salts from the composition of mortars used in past restoration works cannot be disregarded. In future research works, the physicochemical properties of mortars (used in previous restoration works) surrounding each stone ashlar will be studied in order to determine their contribution to weathering and decay of the studied ashlars caused by salt crystallization processes.

Nondestructive techniques such as a simple Karsten pipe to measure hydric behavior or ultrasonic velocity measurements to assess compaction are very useful tools that help to provide on-site results regarding hydric and mechanical properties. These tools give information on the weathering degree, stability, and future evolution of stone building materials, avoiding the sample collection of large quantities of historic construction and building materials. Nevertheless, in-situ analytical methods are considered insufficient to accurately characterize building materials or to identify damage since these show some intrinsic limitations. For example, some sandstones seem to be less weathered because of their highest ultrasonic velocity (V_p) values, but this is caused by the larger amount of salt crystals inside their pore system that cause this parameter to increase, and in fact these display greater decay compared to others with lower V_p values. In general, as mentioned in the literature, the presence of humidity or moisture increases the ultrasonic wave's velocity. Nevertheless, a comparison of the in situ results of both the moisture meter and the ultrasonic waves shows no direct relationship between both parameters since there is no correlation between the values on the superposition of ultrasonic and humidity maps in most of the measured lithotypes. Some sandstones present a high moisture content and high ultrasonic velocity values. This anomaly is attributed equally to the high content of salt crystals and their differential distribution within the rock ashlar. So, it was very difficult to ensure how much moisture content can affect the ultrasonic results in this case because of some parameters that can influence the final results, such as the presence of salt crystals within the porous rock material.

Complementary in-lab microanalyses have allowed a better comprehension of results obtained with nondestructive techniques. The combination of these laboratory analytical techniques reduces the uncertainty of in situ techniques and helps with in situ data interpretation.

The ferruginous red-color sandstone, naturally cemented by iron oxides, offers better possibilities as a high-quality construction material compared to other building materials because of its great strength and durability with higher resistance to the salt crystallization process in coastal areas affected by marine aerosol action.

Acknowledgments

This work was carried out from a collaboration between Universidad Complutense de Madrid (UCM) and the Faculty of Sciences of Bizerte, Tunisia, under the AECID AP/042080/11 project. Laboratory analyses were carried out at Instituto de Geociencias (CSIC, UCM) and were supported by Rafael Fort and the GEOMATERIALES (S2009/MAT-1629) Program. The work was also supported by a JAE-PreDoc 2010-2014 fellowship program of the Spanish National Research Council (CSIC) and the Adaptability and Employment Program of the European Social Fund (ESF 2007-2013). Special thanks go to the technicians Andres Lira and Blanca Gallardo from IGEO (CSIC, UCM) for performing MIP and ion chromatography analyses, and María Ascensión Barajas for the thin sections preparation at the Faculty of Geology (UCM).

References

Alvarez de Buergo, M. (1994). "Estudio del método delamedidadela velocidad de propagación delsonidoysu aplicación aedificios históricos [Study method of measuring the sound propagation speed and its application to historical buildings]." *Ing. Civ.*, 94, 69–74.

Aly, N., Gomez-Herasb, M., Hamed, A., Álvarez de Buergo, M., and Solimane, F. (2015). "The influence of temperature in a capillary imbibition salt weathering simulation test on Mokattam limestone." *Mater. Constr.*, 65(317), 1–11.

Andreini, M., De Falco, A., Giresini, L., and Sassu, M. (2014). "Mechanical characterization of masonry walls with chaotic texture: Procedures and results of in-situ tests." *Int. J. Archit. Herit.*, 8(3), 376–407.

Angeli, M., Bigas, J. P., Benavente, D., Menendez, B., Hebert, R., and David, C. (2007). "Salt crystallization in pores: Quantification and estimation of damage." *Environ. Geol.*, 52, 205–213.

Bouita, H. (1992). *Bizerte: Les monuments islamiques [Bizerte: Islamic monuments]*, Beït Al-Hikma, Carthage, Tunisie (in French).

Bromblet, P., Vergès-Belmin, V., and Simon, S. (2012). "Ultrasonic velocity measurements for the long-term monitoring of the degradation of marble columns in the cloister of the church of Saint-Trophine in Arles (France)." *Proc., 12th Int. Congress on the Deterioration and Conservation of Stone*, Historic Education Preservation Foundation, Washington, DC.

Burkinshaw, R. (2002). "What is the moisture meter trying to tell us?" *Struct. Survey*, 20(5), 162–172.

Calleja, L., Montoto, B., Pérez, B., Suárez del Río, L., Martínez, A., and Menéndez, B. (1989). "An ultrasonic method to analyse the progress of weathering during cyclic salt crystallization laboratory tests." *Proc., 1st Int. Symp. on the Conservation of Monuments in the Mediterranean Basin: The Influence of Coastal Environment and Salt Spray on Limestone and Marble*, Grafo Edizioni, Brescia, Italy, 313–318.

Cardell, C., Benavente, D., and Rodríguez-Gordillo, J. (2008). "Weathering of limestone building material by mixed sulphate solutions: Characterization of stone microstructure, reaction products and decay forms." *Mater. Charact.*, 59(10), 1371–1385.

Croci, G., and Delgado Rodrigues, J. (2002). "Surface and structural stability for the conservation of historic buildings." *Science and technology of the environment for sustainable protection of cultural heritage: EC advanced study course*, Univ. College London, London.

Duarte, E. R., Flores-Colen, I., and De Brito, J. (2011). "In-situ testing techniques for in-service evaluation of water penetration in rendered façades—The portable moisture meter and Karsten tube." *Proc., 12th DBMC Int. Conf. on Durability of Building Materials and Components*, Univ. of Porto, Portugal, 1307–1314.

Esbert, R., Ordaz, J., Alonso, F. J., Montoto, M., González-Limón, T., and Álvarez de Buergo, M. (1997). "Manual de diagnosis y tratamiento de materiales pétreos y cerámicos: Colegio de Aparejadores y Arquitectos Técnicos de Barcelona." *Colección Manuales de Diagnosis*, 5, 139.

Flores-Colen, I., De Brito, J., and Freitas, V. (2011). "On-site performance assessment of rendering façades for predictive maintenance." *Struct. Survey*, 29(2), 133–146.

Fort, R., et al. (2013). "Evolution in the use of natural building stone in Madrid." *Q. J. Eng. Geol.*, 46(4), 421–429.

Fort, R., Fernández-Revuelta, B., Varas, M. J., Alvarez de Buergo, M., and Taborda, M. (2008). "Influence of the anisotropy in the durability of Cretaceous dolostones of the region of Madrid against salt crystallization." *Mater. Constr.*, 58, 74–95.

Gomez-Heras, M., and Fort, R. (2007). "Patterns of halite (NaCl) crystallisation in building stone conditioned by laboratory heating regimes." *Environ. Geol.*, 52(2), 239–247.

Goudie, A. S., (1999). "Experimental salt weathering of limestones in relation to rock properties." *Earth. Surf. Process.*, 24, 715–724.

Gupta, A. S., and Rao, K. S. (1998). "Index properties of weathered rocks: Interrelationships and applicability." *B. Eng. Geol. Environ.*, 57, 161–172.

Herinck, S., De Bouw, M., Pien, A., and Vanhellemont, Y. (2012). "Innovative test procedure on injection products against rising damp for historic masonry constructions." *Proc., Workshop and Training Day*, Oslo, 24–26.

Iñigo, A. C., Alonso, R., and Vicente-Tavera, S. (2001). "Dissolution of salts crystallized in building materials using ultrasound: An alternative to NORMAL (1983) standard methodology." *Ultrason. Sonochem.*, 8, 127–130.

Kahraman, S. (2007). "The correlations between the saturated and dry P-wave velocity of rocks." *Ultrasonics*, 46(4), 341–348.

Kramar, S., Mladenović, A., Kozamernik, M., and Mirtič, B. (2010). "Durability evaluation of some Slovenian building limestones." *Mater. Geoenviron.*, 57(3), 331–346.

López-Arce, P., Doehne, E., Greenshields, J., Benavente, D., and Young, D. (2009a) "Treatment of rising damp and salt decay: The historic masonry buildings of Adelaide, South Australia." *Mater. Struct.*, 42(6), 827–848.

López-Arce, P., Garcia-Guinea, J., Benavente, D., Tormo, L., and Doehne, E. (2009b). "Deterioration of dolostone by magnesium sulphate salt: An example of incompatible building materials at Bonaval Monastery, Spain." *Constr. Build. Mater.*, 23, 846–855.

López-Arce, P., Gomez-Villalba, L. S., Pinho, L., Fernández-Valle, M. E., Álvarez de Buergo, M., and Fort, R. (2010). "Influence of porosity and relative humidity on consolidation of dolostone with calcium hydroxide nanoparticles: Effectiveness assessment with non-destructive techniques." *Mater. Charact.*, 61(2), 168–184.

López-Arce, P., Zornoza-Indart, A., Vázquez-Calvo, C., Gomez-Heras, M., Alvarez de Buergo, M., and Fort, R. (2011). "Evaluation of Portable Raman for the characterization of salt effluorescences at Petra, Jordan." *Spectrosc. Lett.*, 44(7–8), 505–510.

Martinez-Martinez, J., Benavente, D., and García del Cura, M. A. (2011). "Spatial attenuation: The most sensitive ultrasonic parameter for detecting petrographic features and decay processes in carbonate rocks." *Environ. Geol.*, 119, 84–95.

Massari, G., and Massari, I. (1993). "Damp buildings: Old and new Roma." *Int. Centre for the Study of the Preservation and the Restoration of Cultural Property (ICCROM)*, ICCROM, Rome.

Menezes, A. (2012). *In-situ analysis of the physical performance of rendering facades*, Instituto Superior Técnico, Lisbon (in Portuguese).

Menezes, A., Glória Gomes, M., and Flores-Colen, I. (2015). "In-situ assessment of physical performance and degradation analysis of rendering walls." *Constr. Build. Mater.*, 75, 283–292.

Min, K., Park, J., and Han, D. (2005). "Durability of building stones against artificial salt crystallization." *The American Geophysical Union, Fall Meeting*, San Francisco.

Moropoulou, A., Labropoulos, K. C., Delegou, E. T., Karoglou, M., and Bakolas, A. (2013). "Non-destructive techniques as a tool for the protection of built cultural heritage." *Constr. Build. Mater.*, 48, 1222–1239.

Mustoe, G. E. (1982). "The origin of honeycomb weathering." *Geol. Soc. Am. Bull.*, 93, 108–115.

Nwaubani, S. O., and Dumbelton, J. (2001). "A practical approach to in-situ evaluation of surface-treated structures." *Constr. Build. Mater.*, 15, 199–212.

Papida, S., Murphy, W., and May, E. (2000). "The use of sound velocity determination for the non-destructive estimation of physical and microbial weathering of lime- stones and dolomites." *Proc., 9th Int. Congress on Deterioration and Conservation of Stone*, Elsevier, Amsterdam, Netherlands, 609–17.

Paskoff, R., and Sanlaville, P. (1983). "Les côtes de la Tunisie: Variation du niveau marin depuis le Tyrrhénien." Maison de l'Orient, Lyon.

Philippon, J., Jeannette, D., and Lefevre, R. A. (1992). *La conservation de la pierre monumentale en France*. Presse du CNRS, Paris.

Pittarello, L., Bellezza, G., Almesberger, D., and Geometrante, R. (2000). "Anamnesis and diagnosis of column sand capitals of "Nostra Signora delle Grazie" Sanctuary in Imperia (Italy) and quality control of their consolidation by ultrasonic instruments." *Proc., 15th World Conf. on Nondestructive Testing*, Italian Society for Nondestructive Testing and Monitoring Diagnostics-AIPnD, Brescia, Italy, 15–21.

Price, C. A. (1996). "Stone conservation. An overview of current research. Research in conservation." Getty Conservation Institute, Los Angeles.

RILEM. (1980). "Essais recommandés pour mesurer l'altération des pierres et évaluer l'efficacité des méthodes de traitement [Recommended tests to measure the rock weathering and evaluate the effectiveness of treatment methods]." *RILEM 25-PEM*, Berlin, Germany (in French).

Ruedrich, J., and Siegesmund, S. (2007). "Salt and ice crystallisation in porous sandstones." *Environ. Geol.*, 52, 225–249.

Russell, S. A. (1927). *Stone preservation committee report (Appendix I)*, HM Stationary Office, London.

Simon, S. and Lind, A. M. (1999). "Decay of limestone blocks in the block fields of Karnak Temple (Egypt): Nondestructive damage analysis and control of consolidation treatments." *ICOM Committee for Conservation, Triennial Meeting (12th)*, Vol. 2, ICOM, Paris, 743–749.

Surfer 8 [Computer software]. Golden Software, Golden, CO.

Tavares, M., Magalhães, A. C., Veiga, M., and Aguiar, J. (2005). "Diagnosis methods for coatings of ancient buildings: Importance and applicability of in situ tests." *Boletín del Instituto Andaluz del Patrimonio Histórico*, 53, 11–17 (in Spanish).

Török, A. (2003). "Surface strength and mineralogy of weathering crusts on limestone buildings in Budapest." *Build. Environ.*, 38, 1185–1192.

Vallet, J. M., and Vallet-Coulomb, C. (1999). "Characterization of residual efficiency of ancient water repellent products applied on calcareous

stones by using water absorption measurements under low pressure (pipe method)." *Proc., 6th Int. Conf. on Non-Destructive Testing and Microanalysis for the Diagnostics and Conservation of the Cultural and Environmental Heritage*, Istituto Centrale del Restauro, I.C.R, Roma, 417–430.

Vandevoorde, D., et al. (2013). "Validation of in situ applicable measuring techniques for analysis of the water adsorption by stone." *Procedia Chem.*, 8, 317–327.

Van Hees, R., Van Der Klugt, L., De Witte, E., De Clerq, L., Binda, H., and Baronio, G. (1995). "Test methods for the evaluation of the in situ performance of water-repellent treatments." *Proc., 1st Int. Symp. on Surface Treatment of Building Materials with Water Repellent Agents*, Publikatieburo Bouwkunde TU Delft Library, Delft, Netherlands.

Vasconcelos, G., Lourenc, P. B., Alves, C. A. S., and Pamplona, J. B. (2008). "Ultrasonic evaluation of the physical and mechanical properties of granites." *Ultrasonic*, 48(5), 453–466.

Weiss, T., Siegesmund, S., and Rasolofosaon, P. N. J. (2000). "The relationship between deterioration, fabric, velocity and porosity constraint." *Proc., 9th Int. Congress on Deterioration and Conservation of Stone*, Elsevier Science, Amsterdam, Netherlands, 215–223.

Winkler, E. M. (1994). *Stone in architecture, properties, durability*, Springer, Berlin.

Zoghlami, K., and Gómez Gras, D. (2009). "Provenance des roches utilisées dans la construction du Fort d'Espagne de la ville de Bizerte (Tunisie) [Provenance of rocks used in the construction of the Spanish Fort in the city of Bizerte (Tunisia)]." *Proc., Int. Meeting on Architectural Heritage of the Mediterranean*, Lisbon, 48–49 (in French).